Dynamics of semiconductor lasers with optical feedback: Comparison of multimode models in the low-frequency fluctuation regime

I. V. Koryukin
Institute of Applied Physics, Russian Academy of Science, 46 Ulyanov Street, 603950 Nizhny Novgorod, Russia

Paul Mandel
Optique Nonlinéaire Théorique, Universite Libre de Bruxelles, Campus Plaine, C.P. 231, 1050 Bruxelles, Belgium
(Received 17 March 2004; published 19 November 2004)

The role of spontaneous emission noise and gain line profile in the dynamics of a multimode semiconductor laser with weak-to-moderate optical feedback is studied. Two models of such a laser are compared. If the gain profile is flat and in the absence of noise, model A predicts that all modal intensities are in phase, and model B predicts antiphase dynamics of the modal intensities. Noise induces out-of-phase solutions in model A and hardly affects model B. Weakly curved gain profile determines the number of lasing modes but otherwise has little effect on the laser dynamics in both models.

DOI: 10.1103/PhysRevA.70.053819 PACS number(s): 42.55.Px, 42.65.Sf

I. INTRODUCTION

Recent interest in the dynamics of semiconductor lasers with optical feedback is due to the potential applications of such lasers for secure communications by means of chaotic synchronization. The solitary semiconductor laser usually displays stable oscillations with steady intensity as many other class B lasers. External perturbations, such as injected signal, feedback, or pump current modulation, are required to achieve a chaotic output. From a practical viewpoint, optical feedback provided by a backreflecting mirror is one of the simplest ways to achieve chaotic oscillations from a semiconductor laser. Even weak optical feedback leads to complex dynamics [1]. In particular, it can sustain a chaotic regime of low-frequency fluctuations (LFF) with sudden irregular intensity dropouts followed by a gradual intensity recovery [2].

In most analyses published on semiconductor lasers, they are assumed to oscillate on a single longitudinal mode. In this case the dynamics of the semiconductor laser with weak-to-moderate coherent optical feedback is well described by the Lang-Kobayashi equations [3]. However, experiments have demonstrated that many edge-emitting semiconductor lasers with optical feedback are multimode, rather than single mode [4–6], unless frequency selective features are added. Moreover, antiphase mode dynamics was demonstrated in such a laser by comparing the power spectral densities of the total and modal intensities [7]. The presence of antiphase dynamics explains the relative success of the single-mode interpretation [8].

Modeling a multilongitudinal mode semiconductor laser is still an open problem. The dynamics of these lasers depends strongly on the mode-mode coupling in active media, but for semiconductor lasers the nature of the modal interaction is yet unclear. This forces the use of a phenomenological approach to construct models. Two different multimode generalizations of the single-mode Lang-Kobayashi equations were proposed recently. Both use a modal expansion of the electric field but differ in the role of the carrier density. The first type of model uses the assumption that carrier diffusion is very strong and completely washes out the free-carrier density spatial grating burned by the standing-wave pattern of each lasing mode in the Fabry-Perot cavity [9–12]. These models differ in the details of the mode-mode interaction. The mode coupling is treated either as a gain cross-saturation process [11,12] or as a mode-dependent gain [10,13]. The most detailed results on the dynamical behavior for this type of models were obtained for the model introduced in Ref. [10]. We will refer to this model as model A. It was shown analytically that this model has no antiphase solutions branching from the steady intensity solutions [14]. Numerical simulations in the LFF regime display only in-phase and out-of-phase modal dynamics [10]. Another type of multimode extension of the Lang-Kobayashi equations takes into account the free-carrier density gratings associated with the Fabry-Perot configuration [14–16]. The model introduced in Ref. [15] predicts both in-phase and antiphase dynamics [14,15]. We will refer to this model as model B.

Direct comparison of these two models based on previous results is impossible, because different parameters and quite different assumptions were used in the model studies. For instance, model B was studied with the simplifying assumption of equal modal gains (flat gain line profile) and without spontaneous emission noise [14,15]. On the contrary, both a parabolic gain line and a realistic level of spontaneous emission were included in the consideration of model B [10]. The main purpose of this paper is to compare the two multimode models integrated with the same parameters, and to study the role of spontaneous emission noise and gain line profile in the dynamics of the LFF regime.

II. MODEL A

In model A, the slowly varying complex amplitude of the electric field E_m of each lasing mode m is coupled to the spatial average N of the excess free-carrier density

$$\frac{dE_m}{dt} = \frac{1}{2}(1+i\alpha)[G_m(N)-\gamma_m]E_m + k_m E_m(t-\tau_0)e^{-i\omega\tau_0} + F_m(t), \quad (1)$$

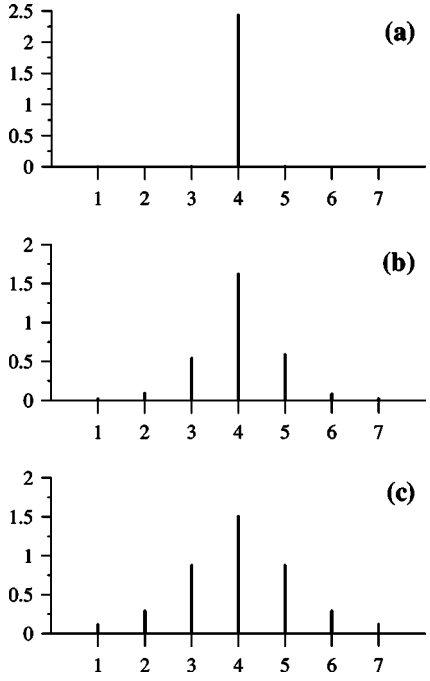

FIG. 1. Optical spectra of the semiconductor laser, calculated by numerical simulation of model A for different rates of spontaneous emission r_{sp}: (a) $r_{sp}=0$; (b) $r_{sp}=10^{-6}$; (c) $r_{sp}=2.5\times10^{-5}$. Other parameters are $\delta=0.022$, $P=10^{-3}$, $\eta=0.0075$, $\tau_0=6$, $\alpha=5$, $T=10^3$, $\beta=0.666$, and $M=7$.

$$\frac{dN}{dt} = J - \frac{N}{\tau_s} - \sum_m^M G_m(N)|E_m|^2, \tag{2}$$

where $G_m(N)=G_c(N-N_0)g_m$ is the modal gain with gain line profile $g_m=1-(m-m_c)^2\delta$, G_c and m_c are the gain coefficient and longitudinal number of gain peak mode, respectively, $\delta=\Delta\omega_L/\Delta\omega_g$, $\Delta\omega_L$ and $\Delta\omega_g$ are the intermode spacing and the active medium gain width, and $N=N_0$ at transparency. The optical modal frequencies are ω_m, α is the linewidth enhancement factor, γ_m is the modal field losses, τ_s is the carrier lifetime, k_m and τ_0 are the modal feedback levels and round-trip time of the feedback loop, and J is the pump current. The mode index m varies from 1 to M, the number of lasing modes. $F_m(t)$ is the Langevin force simulating spontaneous emission noise. The noise level is determined from $\langle F_m^*(t)F_n(t')\rangle=R_{sp}\delta_{mn}\delta(t-t')$. In line with previous simulations, γ_m and k_m are assumed to be mode independent: $\gamma_m\equiv\gamma$ and $k_m\equiv k$.

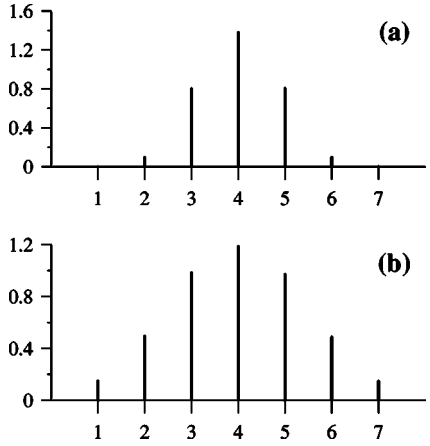

FIG. 2. Optical spectra of the semiconductor laser, calculated by simulation of model B: (a) $r_{sp}=0$; (b) $r_{sp}=2.5\times10^{-5}$. Other parameters as in Fig. 1.

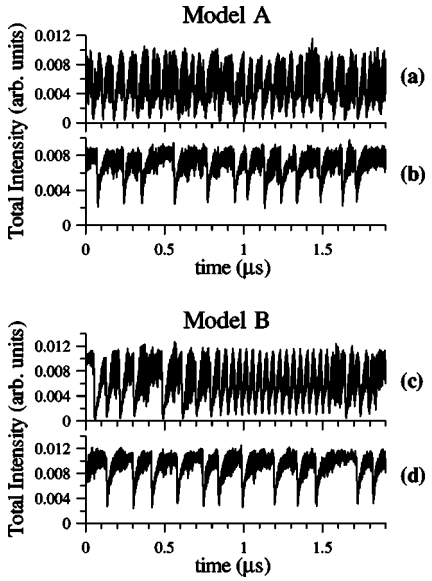

FIG. 3. Averaged total laser intensity in the LFF regime for the two models: (a) and (c) $r_{sp}=0$; (b) and (d) $r_{sp}=2.5\times10^{-5}$. Other parameters as in Fig. 1.

With standard normalization, similar to that used for model B [15], the normalized equations of model A become

$$\frac{dA_m}{d\tau} = (1+i\alpha)\left(g_m D - \frac{1-g_m}{2}\right)A_m + \eta A_m(\tau-\tau_0) \times e^{-i\omega_m\tau_0} + f_m(\tau), \tag{3}$$

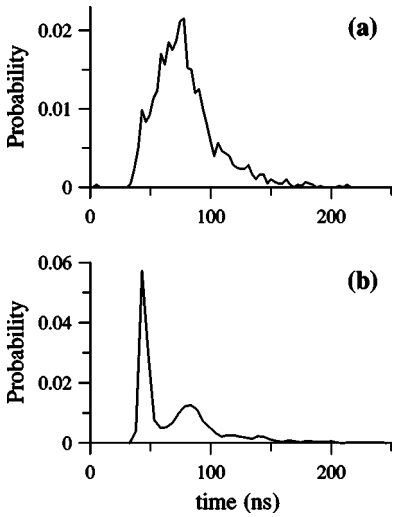

FIG. 4. Probability distribution function of the time interval between two consecutive dropouts for model A (a) and model B (b) from simulations without spontaneous noise, $r_{sp}=0$, other parameters as in Fig. 1.

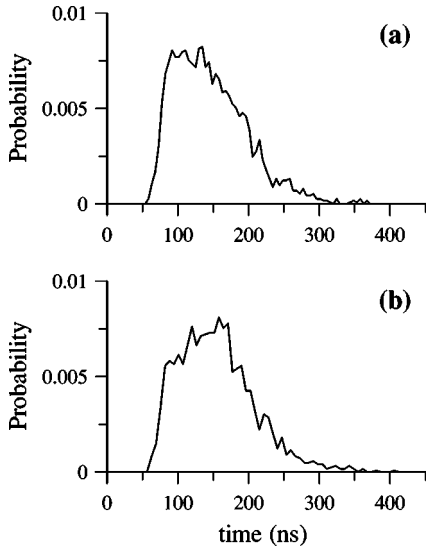

FIG. 5. Same as Fig. 4, but with spontaneous noise, $r_{sp}=2.5\times10^{-5}$.

$$T\frac{dD}{d\tau}=P-D-(1+2D)\sum_{n}^{M}g_n|A_n|^2, \tag{4}$$

where the dimensionless variables and parameters are defined as

$$A_m=\sqrt{G_c\tau_s/2}E_m,\quad D=G_c(N-N_{th})/2\gamma,\quad \tau=\gamma t,$$

$$N_{th}=N_0+\gamma/G_c,\quad P=\frac{G_c}{2\gamma}(J-J_{th})/J_{th},\quad J_{th}=N_{th}/\tau_s,$$

$$T=\gamma\tau_s,\quad \eta=k/\gamma.$$

The normalized level of spontaneous emission noise $f_m(\tau)$ is $r_{sp}=R_{sp}\sqrt{\tau_s/2}/\gamma$.

III. MODEL B

In this model the set of nonlinear modal gains N_m is used instead of the space average N. The N_m include both the uniform component and spatial gratings of the free-carrier density. Taking into account gain line profile and spontaneous emission noise we can write the model B equations as

$$\frac{dE_m}{dt}=\frac{1}{2}(1+i\alpha)(g_mN_m-\gamma_m)E_m+k_mE_m(t-\tau_0)\times e^{-i\omega_m\tau_0}+F_m(t), \tag{5}$$

$$\frac{dN_m}{dt}=J-\frac{N_m}{\tau_s}-N_m\sum_{n}^{M}g_n\beta_{mn}|E_n|^2. \tag{6}$$

The phenomenological cross-saturation parameters $0<\beta_{nm}<1$ measure the mode-mode coupling due to carrier density gratings. They are assumed to be mode independent: $\beta_{nm}=\beta$ for $m\neq n$, and $\beta_{mm}=1$. The other parameters have the same meaning as for the first model.

After normalization, the equations of model B become

$$\frac{dA_m}{d\tau}=(1+i\alpha)\left(g_mD_m-\frac{1-g_m}{2}\right)A_m+\eta A_m(\tau-\tau_0)e^{-i\omega_m\tau_0}+f_m(\tau), \tag{7}$$

$$T\frac{dD_m}{d\tau}=P-D_m-(1+2D_m)\sum_{n}^{M}g_n\beta_{mn}|A_n|^2, \tag{8}$$

where the dimensionless variables and parameters are defined as

$$A_m=\sqrt{\tau_s/2}E_m,\quad D_m=(N_m-\gamma)/2\gamma,\quad P=(J-J_{th})/2J_{th},$$

$$J_{th}=\gamma/\tau_s.$$

IV. COMPARISON OF THE TWO MODELS

For a small feedback coefficient η, both models have stable steady-state solutions. However, as η is increased, these steady-state solutions are destabilized via completely different mechanisms [14]. Model A exhibits only a standard self-pulsing instability through a nondegenerate Hopf bifurcation associated with the in-phase relaxation oscillation frequency f_R, which is very close to the single-mode relaxation oscillation frequency. In model B, this instability is also possible. But there is an additional instability, a degenerate Hopf bifurcation, associated with the low relaxation oscillation frequency f_L given by $f_L^2=f_R^2(1-\beta)/[1+\beta(M-1)]<f_R^2$. This bifurcation can generate coexisting periodic and quasiperiodic attractors that display antiphase dynamics [14,17].

For numerical simulation of Eqs. (3), (4) and Eqs. (7), (8), we chose two sets of laser parameters corresponding to the

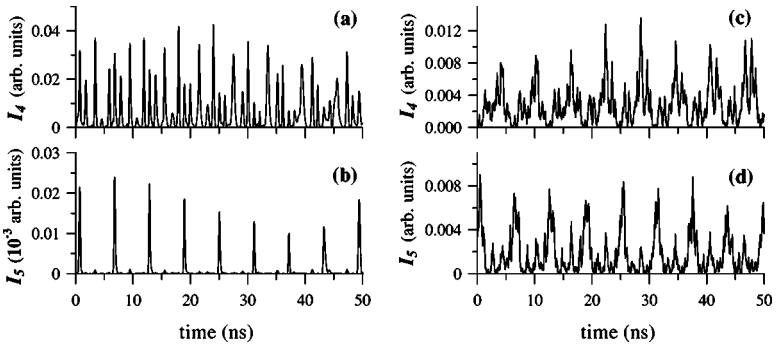

FIG. 6. Modal intensities for model A: (a) and (b) correspond to Fig. 3(a) ($r_{sp}=0$), and (c) and (d) correspond to Fig. 3(b) ($r_{sp}=2.5\times10^{-5}$).

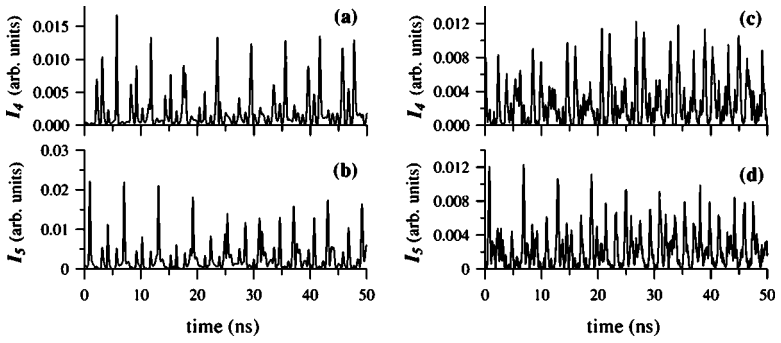

FIG. 7. Same as in Fig. 6, but for model B: (a),(b) $r_{sp}=0$; (c),(d) $r_{sp}=2.5\times10^{-5}$.

parameters used in Refs. [10,15] and leading to the LFF regime: $P=10^{-3}$, $\eta=0.0075$, and $\tau_0=6$ for the parameters of Ref. [15], and $P=0.12$, $\eta=0.077$, and $\tau_0=3$ for the parameters of Ref. [10]. The common parameters are $\alpha=5$, $T=10^3$, $\beta=0.666$, and $M=7$. The first set of parameters is used in this paper for all the figures, while the second set of parameters is used for the table.

Spontaneous emission noise plays a key role in model A: this noise is the main cause of cavity multimode oscillations themselves since, without it, the only stable regime predicted by the model is single-mode oscillation. Spontaneous emission leads to changes in the optical spectrum involving sideband modes in the lasing regime (Fig. 1). On the contrary, the multimode behavior of model B is due to the spatial gratings of the population inversion and depends weakly on the level of spontaneous noise (Fig. 2) even for a sufficiently high value of the gain profile parameter δ.

The effect of the spontaneous emission noise on the total intensity is quite similar for the two models. LFF regime without spontaneous noise is slightly different in the both models. The main difference is in quasiregular dropouts suddenly appearing in the time trace of model B averaged intensity, which are absent in model A [Figs. 3(a) and 3(c)]. Outside these intervals, the temporal wave forms are very similar in both models. Such behavior leads to different probability distribution functions of the interval between consecutive dropouts, namely to a narrow sharp peak for model B (Fig. 4). Spontaneous noise leads to an increase of the average time between intensity dropouts, to a decrease of both the oscillation amplitude during the recovery process and the dropouts' depth, i.e., to a more regular LFF regime [Figs. 3(b) and 3(d)]. Periods of quasiregular LFF in the model B intensity disappear if noise is included. Probability distribution functions have the same shape for both models and display only one broad peak (Fig. 5). This dropout statistic is similar to that calculated in the single-mode case [18].

However, the modal intensities are quite different for the two models. Without spontaneous emission noise, model A supports only in-phase oscillations for all lasing modes. Spontaneous emission changes this behavior and gives rise to out-of-phase modal dynamics (Fig. 6). On the contrary, model B predicts antiphase oscillations even without noise. A modal dependence of the gain profile does not destroy this behavior if the value of δ allows more than one mode to oscillate. The spontaneous emission noise leads only to quantitative changes of the antiphase behavior (Fig. 7).

It was shown [19] that antiphase dynamics could be inferred from the relations between power spectral densities (PSD) of the total and modal intensities. This approach was recently refined and applied experimentally [7]. Let $P(I_j,f)$ and $P(\Sigma I,f)$ be the PSD of the jth modal intensity and of the total intensity at frequency f. The relations can be expressed as follows: perfect in phase:

$$P(\Sigma I,f)=\left[\sum\sqrt{P(I_j,f)}\right]^2, \tag{9}$$

perfect in antiphase:

$$P(\Sigma I,f)=0, \tag{10}$$

partial antiphase:

$$\sum P(I_j,f)>P(\Sigma I,f)>0. \tag{11}$$

Frequency ranges where the condition of partial antiphase behavior (11) is satisfied are presented in Table I together with a value of the relaxation oscillation frequencies. The results are obtained for the set of parameters used in Ref. [10]. For both models, without spontaneous emission noise, relation (9) is verified in the vicinity of the in-phase relaxation oscillation frequency, indicating perfect in-phase dynamics at these frequencies. Partial antiphase (out-of-phase) behavior is present only at the low frequencies corresponding to the inverse feedback roundtrip time 0.35 GHz. For a

TABLE I. Frequency ranges where partial antiphase occurs using $P=0.12$, $\eta=0.077$, $\tau_0=3$, and the parameters of Ref. [10].

		Model A	Model B
In-phase relaxation oscillations frequency		$f_R=3.1$ GHz	
Antiphase relaxation oscillations frequency		no	$f_L=0.83$ GHz
Antiphase behavior	$r_{sp}=0$	$f<0.35$ GHz	$f<1.5$ GHz
	$r_{sp}=2.5\times10^{-5}$	$f<0.9$ GHz	$f<1.5$ GHz

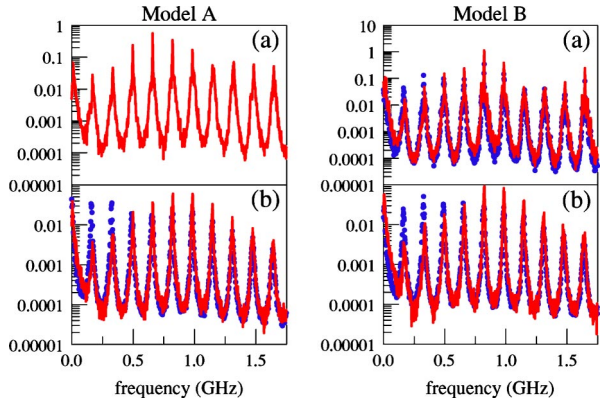

FIG. 8. (Color online) Power spectral density $P(\Sigma I, f)$ of the total intensity (continuous curve) and incoherent sum $\Sigma P(I_j, f)$ of the modal power spectral densities (dotted line) as a function of frequency. Antiphase dynamics occurs in the range where $\Sigma P(I_j, f) > P(\Sigma I, f)$. Same parameters as in Figs. 6 and 7.

realistic level of spontaneous noise, the upper boundary of this behavior shifted close to 1 GHz, indicating the significant role of spontaneous noise for the appearance of the antiphase dynamics. On the contrary, model B displays antiphase behavior even without noise, in the frequency range below the low relaxation oscillation frequency. The effect of spontaneous emission noise manifests itself only by small quantitative changes of this behavior. For completeness, we also display in Fig. 8 the PSD of the total intensity (continuous line) and the incoherent sum $\Sigma P(I_j, f)$ (dotted line). Antiphase dynamics, which implies the inequality $\Sigma P(I_j, f) > P(\Sigma I, f)$, occurs in the low-frequency regime except for the deterministic version of model A. It is interesting to note that the use of the PSD only allows to state that the multimode dynamics is not in phase. It does not distinguish between the out-of-phase regime and the wealth of antiphase regimes described, e.g., in Refs. [17,20].

V. CONCLUSION

We have investigated numerically the dynamical behavior of two multimode models of a semiconductor laser with weak-to-moderate optical feedback in the LFF regime. Spontaneous emission noise plays a key role in the dynamics of model A. Spontaneous noise leads to changes in the modal spectrum involving sideband modes in the lasing regime. Moreover, out-of-phase modal behavior is due to spontaneous emission noise only. On the contrary, antiphase behavior of model B has a dynamical origin and exists even without noise. The effect of spontaneous emission manifests itself only in small quantitative changes of this behavior. The gain line profile leads to a decrease of the sideband mode intensities and plays a minor role in the laser dynamics for the both models. Let us mention that without external feedback but for much higher current ($J = 2J_{th}$) than those where LFF is usually observed, antiphase dynamics and full compensation have been observed in the numerical simulation of a simplified rate equation model that accounts for cross- and self-saturation [21].

Models A and B are not the only attempts to describe the dynamical behavior of multimode semiconductor lasers in Fabry-Perot resonators with external feedback. The main other class of models are the so-called propagation models which do not rest on a modal expansion of the electric field, but deal directly with partial differential propagation equations for the electric field. The relation between microscopic modeling and these mean-field models has been summarized in Ref. [22]. A two-level-like mean-field propagation model has been analyzed [23], while a more systematic study of the power output of a multimode semiconductor laser has recently been published [24]. Noise has also been modeled with partial differential equations for more complex types of lasers, such as a three-section laser comprising two distributed feedback sections, detuned by the stop band width, and enclosing an integrated phase detuning section [25]. However, these papers do not analyze the influence of noise on the modal antiphase dynamics. An exception is the experimental work reported in Ref. [4], where out-of-phase dynamics is reported for two dominant modes. However, the case of two modes is degenerate and cannot be used to discriminate between out-of-phase and antiphase dynamics.

ACKNOWLEDGMENTS

This research was supported by the Russian Foundation for Basic Research (Grant No. 03-02-17243), the Russian President Program for Support of Scientific Schools (Grant No. 1622.2003.2), the Fonds National de la Recherche Scientifique, and the Interuniversity Attraction Poles Program–Belgian Science Policy.

[1] K. Petermann, IEEE J. Sel. Top. Quantum Electron. **1**, 480 (1995).
[2] T. Morikawa, Y. Mitsuhashi, and J. Shimada, Electron. Lett. **12**, 435 (1976).
[3] R. Lang and K. Kobayashi, IEEE J. Quantum Electron. **16**, 347 (1980).
[4] G. Huyet *et al.*, Phys. Rev. A **60**, 1534 (1999).
[5] G. Huyet *et al.*, Opt. Commun. **149**, 341 (1998).
[6] G. Vaschenko *et al.*, Phys. Rev. Lett. **81**, 5536 (1998).
[7] A. Uchida, Y. Liu, I. Fischer, P. Davis, and T. Aida, Phys. Rev. A **64**, 023801 (2001).
[8] P. Mandel, E. A. Viktorov, C. Masoller, and M. S. Torre, Physica A **327**, 129 (2003).
[9] J. Mørk, B. Tromborg, and P. L. Christiansen, IEEE J. Quantum Electron. **24**, 123 (1988).
[10] F. Rogister, P. Megret, O. Deparis, and M. Blondel, Phys. Rev. A **62**, 061803 (2000).
[11] A. T. Ryan, G. P. Agrawal, G. R. Gray, and E. C. Gage, IEEE J. Quantum Electron. **30**, 668 (1994).
[12] D. W. Sukow *et al.*, Phys. Rev. A **60**, 667 (1999).

[13] J. M. Buldu *et al.*, J. Opt. B: Quantum Semiclassical Opt. **4**, 415 (2002).
[14] T. W. Carr, D. Pieroux, and P. Mandel, Phys. Rev. A **63**, 033817 (2001).
[15] E. A. Viktorov and P. Mandel, Phys. Rev. Lett. **85**, 3157 (2000).
[16] M. Yousefi *et al.*, IEEE J. Quantum Electron. **39**, 1229 (2003).
[17] A. G. Vladimirov, E. A. Viktorov, and P. Mandel, Phys. Rev. E **60**, 1616 (1999).
[18] W.-S. Lam, P. N. Guzdar, and R. Roy, Int. J. Mod. Phys. B **17**, 4123 (2003).
[19] P. Mandel and J.-Y. Wang, Phys. Rev. Lett. **75**, 1923 (1995); **76**, 1403(E) (1996).
[20] J. Y. Wang and P. Mandel, Phys. Rev. A **52**, 1474 (1995).
[21] M. Ahmed and M. Yamada, IEEE J. Quantum Electron. **38**, 682 (2002).
[22] P. Ru, J. V. Moloney, and R. Indik, Phys. Rev. A **50**, 831 (1994).
[23] M. Homar, J. V. Moloney, and M. San Miguel, IEEE J. Quantum Electron. **32**, 553 (1996).
[24] C. Serrat, S. Prins, and R. Vilaseca, Phys. Rev. A **68**, 053804 (2003).
[25] H.-J. Wünsche, M. Radziunas, S. Bauer, O. Brox, and B. Sartorius, IEEE J. Sel. Top. Quantum Electron. **9**, 857 (2003).